JOURNAL OF MATERIALS SCIENCE 10 (1975) 427–435

The influence of pressurization-induced dislocations on the plastic deformation of LiF and NaCl monocrystals

R. A. EVANS*, A. S. WRONSKI, B. A. W. REDFERN
School of Materials Science, University of Bradford, West Yorkshire, UK

Single crystals of LiF containing voids and of NaCl containing Na_2SO_4 precipitates were pressurized to introduce dislocations in the vicinities of the discontinuities and subsequently compressed along ⟨100⟩ at room temperature. The yield stress was raised in both materials; additionally, in LiF discontinuous yielding and easy glide were suppressed and work hardening rate increased by the pressurization-induced dislocations. Following pressurization at 0.85 GN m^{-2}, for example, the 0.1% shear flow stress of LiF was doubled to $\sim$ 4 MN m^{-2} and stage II work hardening rate quadrupled to $\sim$ 180 MN m^{-2}. Pressurization of NaCl above 0.6 GN m^{-2} resulted in an increase in the 0.1% flow stress from $\sim$ 1.2 to $\sim$ 2.0 MN m^{-2}. If the slip bands in LiF were initiated by a precompression, pressurization prevented the broadening of these fresh slip bands during subsequent plastic flow. Deformation now took place at a higher stress both in LiF and NaCl. These effects resemble in some ways latent hardening in that oblique as well as conjugate dislocation intersections must take place to continue the deformation. In contrast to latent hardening data, the strain hardening rate was increased in LiF and was approximately proportional to the pressurization-induced dislocation density. This ratio, 5 to 6 dyne per dislocation, is in fair agreement with two sets of independent calculations reported by Gilman and Johnston. The results suggest, therefore, that in the present case also hardening may be due to defects left in the wakes of pressurization-induced moving dislocations.

1. Introduction

When single crystals possessing the rock-salt structure are compressed along ⟨100⟩, four ⟨110⟩ {110} slip systems are equally stressed [1-3]. Usually, however, slip commences on two orthogonal systems – the primary pair – and when one of these becomes inactive a linear stress-strain curve results [1]. The two inactive systems, oblique to the first pair, are nevertheless hardened by the primary slip; this phenomenon is called latent hardening. It has been investigated in the alkali halides [3-7] simply by compressing single crystals along one ⟨100⟩ direction and then measuring the flow stress on the previously inactive, i.e. latent, oblique system by compressing in a second (hard) cube direction parallel to the primary planes. The increase in flow stress, by factors of up to 14 in LiF and 9 in NaCl [3], has been associated with the interaction of glide dislocations in the latent slip system with dipoles and dislocations in the primary system, tentatively according to the reaction [6, 7]:

$$\frac{a}{2}[110] + \frac{a}{2}[\bar{1}0\bar{1}] \rightarrow \frac{a}{2}[01\bar{1}]. \qquad (1)$$

The work hardening rates on the latent system in both NaCl and LiF were approximately zero and Li [6] associated the propagation of a dislocation band in these circumstances to that of a Lüders band. It was found, however, that an enhanced rate of hardening, at a reduced flow stress, results if the latent hardened crystal is annealed. He associated this phenomenon with the dislocation distribution after recovery: reduced dislocation density and dispersed dislocation bands. Surprisingly for LiF, uniform

*Present address: Synthetic Fibres Division, Courtaulds Ltd, Coventry CV6 5AE, UK.

distribution of dislocations is reported after compression only in the primary direction both by Li [6] and Nakada and Keh [7], in contrast to the glide bands commonly observed [8].

Latent hardening experiments on the alkali halides [3-7] have thus been concerned with the mechanisms of plastic deformation when oblique systems interact. Another means of modifying the microstructure so as to force oblique interactions during simple compression is the pressurization of materials containing elastic discontinuities [9-11]. Subjecting monocrystals containing these discontinuities (voids in LiF and Na_2SO_4 precipitates in NaCl) to hydrostatic pressures of the order of 1 GN m^{-2} results in matrix shear stresses at the interfaces sufficient for dislocation generation, frequently in *all* the $\langle 110 \rangle$ $\{110\}$ slip systems [11] of the rock salt structure. It has also been suggested that interactions given by Relation 1 for latent hardening already take place during pressurization of LiF [11] and MgO [12]. The microstructure thus produced contrasts to that introduced by simple precompression and should accordingly differently influence the mechanical properties subsequently determined at atmospheric pressure.

In principle, the pressurization-induced dislocations can both move to cause plastic deformation – thereby lowering the yield stress, as in e.g. body-centred cubic metal and NaCl polycrystals [12-15] – or act as a forest to gliding dislocations – thereby increasing the flow stress, as e.g. in monocrystalline chromium [16]. In general, in monocrystals the problem of maintaining continuity of strain and stress across grain boundaries does not arise and, therefore, in contrast to the results on polycrystalline NaCl [15], pressurization-induced hardening is expected.

2. Experimental techniques

The materials, preparation, polishing and repeated etching techniques have been described previously [9, 11]. The presence of 3500 ppm of Na_2SO_4 in the AnalaR NaCl melt resulted in randomly distributed, approximately spherical, particles of thenardite 5 to 35 μm in diameter. To produce voids the Quartz et Silice LiF monocrystals were irradiated to an integrated neutron flux of 8×10^{16} nvt* (in the DIDO reactor at AERE, Harwell), annealed at $\sim$ 800°C in a sealed evacuated silica tube for 20 h and slowly cooled. The cubical voids, of various aspect ratios, had edge lengths extending to $\sim$ 100 μm.

In LiF many of the cavities were associated with subgrain boundaries, but those in the matrix were dislocation free [11]. The mean dislocation densities, estimated from etch pit counts on $\{100\}$ faces, were 1 to 2×10^5 cm^{-2}. In the NaCl as-cooled crystals, however, these mean values were 5×10^5 to 3×10^6 cm^{-2} and many of the dislocations were associated with the Na_2SO_4 particles [9].

Pressurizations, in the range 0.1 to 1.5 GN m^{-2}, were carried out either in isopentane or hydraulic oil in a NPL-type piston-cylinder apparatus. Unpressurized and pressurized specimens, of approximate dimensions 10 mm × 2 mm × 2 mm and of $\langle 100 \rangle$ orientation, were compressed at room temperature in a modified Hounsfield tensometer at rates of $\sim 2 \times 10^{-4}$ sec^{-1}. Some samples were strained, unloaded, pressurized and retested.

3. Pressurization-induced microstructures

In the LiF crystals nucleation of dislocations in the vicinities of the cubical holes was observed (using the repeated etching technique) above threshold pressures $\geqslant 0.1$ GN m^{-2}, characteristic of the cavity size. On raising the pressure, further dislocations were generated [11]. The dislocation arrays were on the twelve $\langle 110 \rangle$ $\{110\}$ slip systems, each being associated with a cavity edge. A mechanism for this pressurization-induced dislocation nucleation suggests not prismatic punching, but a slip process [11, 12], whereby one or more pairs of half-loops is generated by each cavity edge on a $\{110\}$ plane containing or adjacent to that edge. The stability and ultimate arrangement of the dislocation structures (Fig. 1a) depends on pressure and this is schematically represented in Fig. 1b. The maximum pressure reached during the seasoning treatment, together with the cavity size and shape, determines the local strains and shear stresses responsible for dislocation generation and, subsequently, the probability of cross-slip and dislocation interactions. Dislocation arrays resulting from a given pressurization are stable in this LiF, as, e.g. treatment at a higher pressure produces fresh dislocations and no discernible movement of dislocations in existing

*nvt = neutron velocity time.

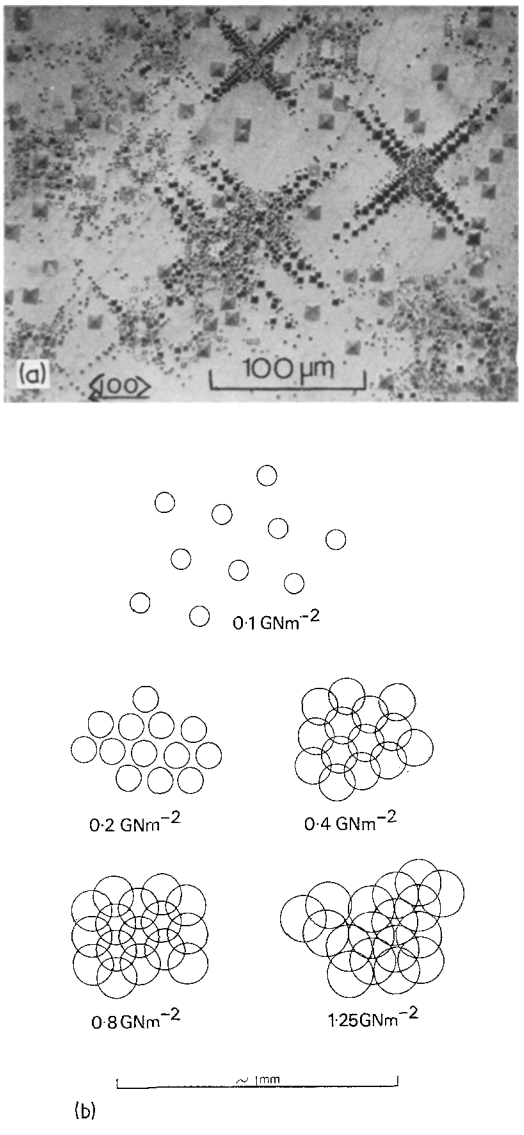

Figure 1 (a) The development of well defined dislocation arrays (detected by successive etching of a {100} plane) around cavities in a LiF monocrystal following treatments at 0.1, 0.2, 0.4, 0.8 and 1.25 GN m^{-2}. The pit size depends on the number of etching operations, i.e. the largest pits correspond to the dislocations present before pressurization and the smallest to dislocations generated at 1.25 GN m^{-2}. Note that the number of active sources and the dislocation density markedly increase with pressure. (b) Schematic two-dimensional representation of the increasing localized plastic deformation following the above series of pressurizations. The diameters of the circles correspond to the average dislocation array size and the spacing of the centres to the average spacing of sources at each pressure. (These islands are the barriers to slip band formation.)

planes [11]. In general, however, the development of the pressurization-induced arrays appears similar to the mechanism of conventional slip band broadening [8].

Microscopic examination of etched {100} faces of LiF showed that the dislocation density increased approximately linearly with pressure: from $\sim 9 \times 10^5$ to $\sim 5 \times 10^6$ cm^{-2} as the treatment varied from 0.2 to 1.25 GN m^{-2} [10]. In NaCl, however, no effects of pressurization were detected below 0.6 GN m^{-2}, but at higher pressures [9] dislocations were generated, sometimes in complex arrays, in the vicinities of the precipitate particles. The simple Brooks [17] criterion predicts the generation of 20 to 140 loops in each of the twelve $\langle 1\,1\,0 \rangle$ directions at a pressure of 0.6 GN m^{-2}, about 720 per particle of 15 μm diameter. If all the Na_2SO_4 is assumed to be in the form of such spheres, the pressurization-induced dislocation density evaluates then to $\sim 4 \times 10^6$ cm^{-2}. The presence of existing dislocations, however, particularly in the vicinities of the precipitate particles, is thought to complicate the pressurization-induced microstructure in the NaCl matrix. As these pre-pressurization densities ranged up to $\sim 3 \times 10^6$ cm^{-2} the total is thought to be in fair agreement with the total densities of $\sim 10^7$ cm^{-2} estimated for pressurizations at > 0.6 GN m^{-2}. Although these calculations for NaCl are approximate, this correlation, with reference to the quantitatively studied LiF, offers encouraging support for the mechanisms proposed for LiF and MgO [11, 12].

4. Compression testing of NaCl

The shear stress for macroscopic plastic flow (i.e. at 0.1% plastic strain), τ_y, of the as-cooled crystals ranged from 1.0 to 1.3 MN m^{-2}. Treatments at 0.25, 0.5 and some at 0.6 GN m^{-2} did not detectably effect τ_y. These results are presented in Fig. 2 together with those for the 0.7, 1.0 and 1.5 GN m^{-2} pressurizations. It is seen that the mean τ_y for specimens treated at these higher pressures (and some at 0.6 GN m^{-2}) had been raised to 1.9 MN m^{-2}, i.e. by $\sim 60\%$. In spite of the large scatter in τ_y, statistical analysis has shown the threshold to be significant at better than the 0.1% level. It should be noted that this threshold corresponds approximately to the pressure below which no dislocation generation was observed in this material.

Pressurization at 1 GN m^{-2} of $NaCl/Na_2SO_4$ crystals previously subjected to 1 to 2% strain resulted in increases in the flow stress of $\sim 10\%$

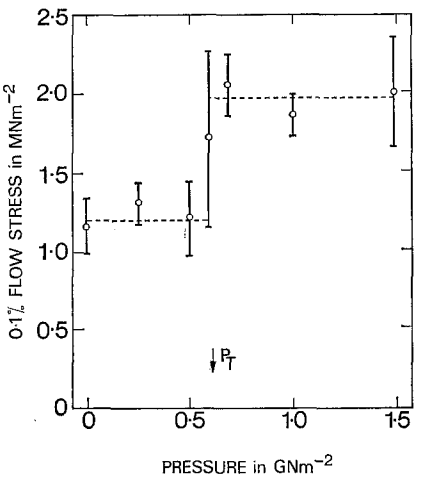

Figure 2 The pressurization treatment dependence of the 0.1% flow stress, determined at room temperature at a compressive rate of $\sim 2 \times 10^{-4}$ sec^{-1}, of NaCl single crystals containing Na_2SO_4 precipitates.

when the straining was continued (Fig. 3b). This behaviour contrasts with similar tests of polycrystalline samples [15] when decreases in the flow stress were observed. No effect of the unload/reload cycle on the flow stress was detected, indicating the reliability of the testing procedure. When NaCl monocrystals (containing $\sim$ 60 ppm Cd and devoid of detectable precipitates) were strained, pressurized and retested, no changes in the flow stress (Fig.) 3a were observed.

5. Compression testing of LiF

Unpressurized LiF crystals exhibited yield drops and easy glide occurred at a shear stress of $\sim$ 2 MN m^{-2} (e.g. Fig. 4a). These phenomena were suppressed by treatments at the lowest hydrostatic pressure employed, 0.2 GN m^{-2}, and Fig. 4b and c show the initial parts of the stress-strain curves of specimens pressurized at 0.4 and 0.85 GN m^{-2}, respectively. It is seen that pressurization also produces significant increases in the yield stress of the specimens. A graph of 0.1% proof stress, τ_y, versus soaking pressure (Fig. 5) shows this relationship to be approximately linear with a slope of $\sim$ 2 MN m^{-2} per GN m^{-2} of seasoning pressure for the range extending to 0.85 GN m^{-2}. It is seen that the specimen tested following pressurization at 0.85 GN m^{-2} exhibited nearly twice the yield strength of the unpressurized crystals. The transition between the elastic and microstrain region and the linear work hardening region of the stress-strain curves of the pressurized specimens (shown in Fig. 4) occupied stress increments of approximately 0.5 and 1.0 MN m^{-2} for the 0.4 and 0.85 GN m^{-2} pressurizations, respectively. The work hardening rate in stage II was also increased by the pressurization treatments; the variation was again approximately linear (Fig. 6). Specimens pressurized at e.g. 0.85 GN m^{-2} exhibited thus work hardening rates approximately four times those of unpressurized crystals, $\sim$ 40 MN m^{-2}.

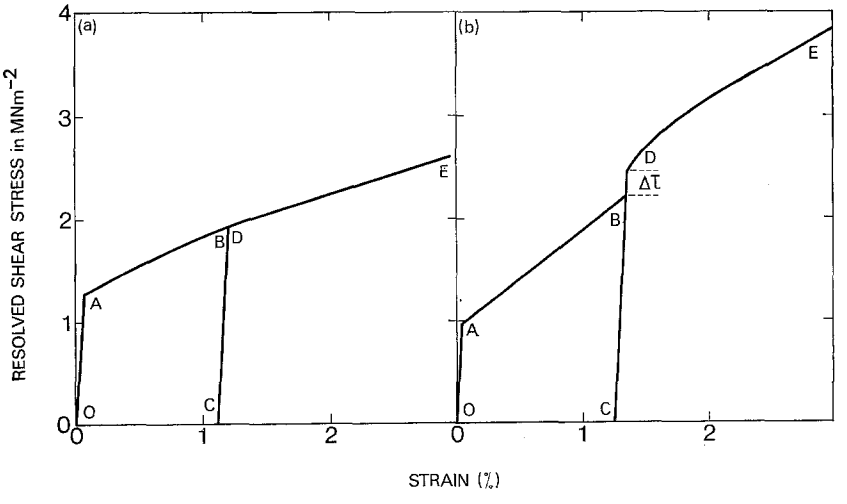

Figure 3 The stress-strain dependence, at room temperature and compressive strain rate of $\sim 2 \times 10^{-4}$ sec^{-1}, of NaCl monocrystals containing: (a) Cd in solution and (b) Na_2SO_4 precipitates. The specimens were loaded: OAB, unloaded; BC, pressurized at 1 GN m^{-2} and reloaded: CDE. Note the stress increase $\Delta\tau$ in (b) only.

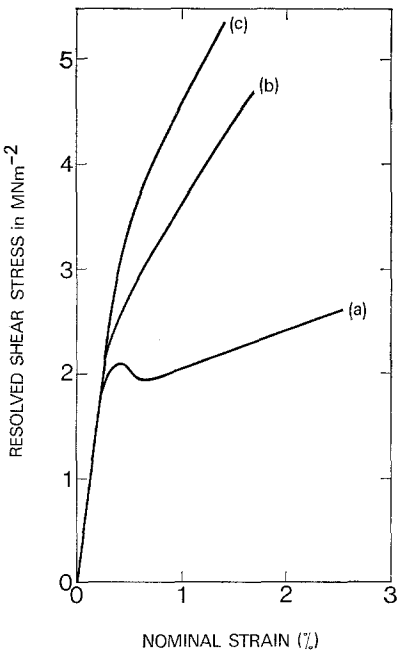

Figure 4 Stress strain curves for LiF single crystals containing cubical cavities compressed at room temperature at a rate of $\sim 2 \times 10^{-4}$ sec^{-1} in (a) unpressurized state and (b) and (c) following pressurizations at 0.4 and 0.85 GN m^{-2} respectively.

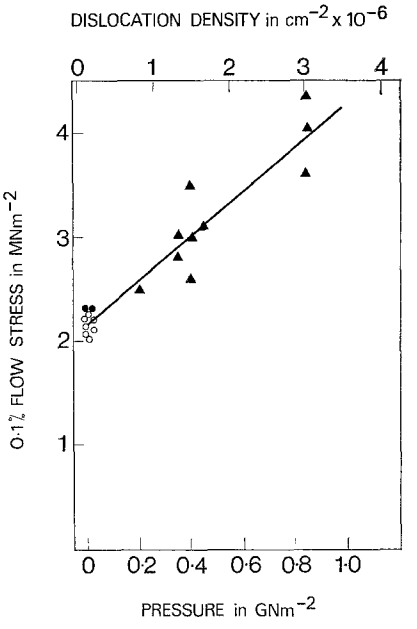

Figure 5 The pressurization treatment dependence of the 0.1% flow stress, determined at room temperature at a compressive rate of $\sim 2 \times 10^{-4}$ sec^{-1}, of LiF single crystals containing cubical cavities. Note that the pressurization-induced dislocation density is also indicated on the abscissa [11]. Full symbols refer to unpressurized specimens which were deliberately mishandled.

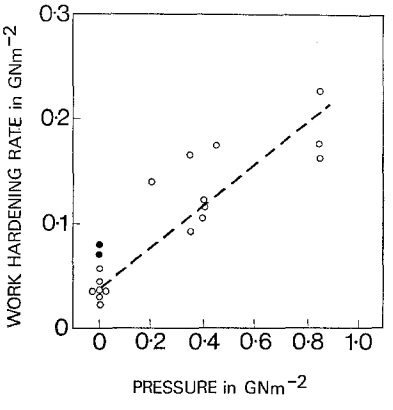

Figure 6 The variation of the work hardening rate of LiF single crystals containing cavities with the pressurization treatment. Compression tests were performed at room temperature at a rate of $\sim 2 \times 10^{-4}$ sec^{-1}. Full symbols refer to deliberately mishandled unpressurized specimens.

The scatter in the values of the yield stress and work hardening rate for the unpressurized specimens was $\pm$ 0.15 and $\pm$ 20 MN m^{-2}, respectively; it was increased substantially, i.e. to $\pm$ 0.45 and $\pm$ 35 MN m^{-2}, following pressurization. It should be noted, however, that for two deliberately "mishandled", but unpressurized, specimens (referred to by full symbols on Figs. 5 and 6) yield drops and easy glide regions were replaced by only points of inflection on the stress-strain curves. This considerable damage also had no appreciable effect on the subsequent work hardening rate.

To study the relative contributions to plastic deformation of pressurization-induced and compression-induced dislocations, the deformation of an unpressurized LiF specimen was interrupted at a strain of 0.5%, the crystal was removed and subjected to a "dummy" (i.e atmospheric) pressurization treatment and reloaded. No change in flow stress or work hardening rate was detected (Fig. 7). The specimen was then taken through another unload–pressurize–reload cycle following a further 0.4% strain, which this time included a genuine treatment at 0.75 GN m^{-2}. On loading the stress necessary to reinitiate plastic flow was seen to increase by $\sim$ 15% and the new work hardening rate by $\sim$ 2. This type of test was carried out on several other specimens and all the results are similar.

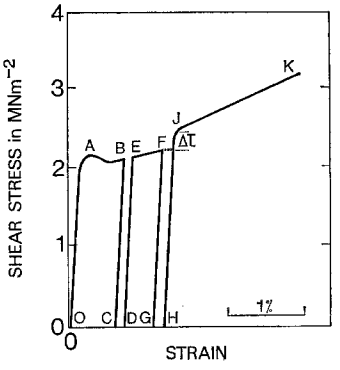

Figure 7 The stress-strain dependence, at room temperature and compressive rate of $\sim 2 \times 10^{-4}$ sec^{-1} of LiF single crystal containing cavities which was loaded: OAB, unloaded: BC, reloaded: DEF, unloaded: FG, pressurized at 0.75 GN m^{-2} and again loaded: HJK. Note the stress increase $\Delta\tau$ between F and J only and the accompanying increase in the work hardening rate.

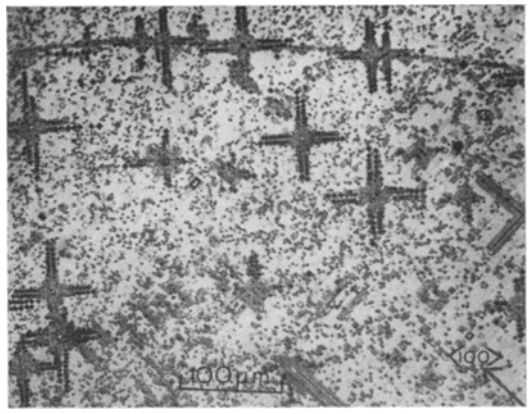

Figure 8 The microstructure on a {100} face (on which edge slip bands would normally form) of a pressurized LiF monocrystal containing cavities compressed at room temperature 0.6% at a rate of $\sim 2 \times 10^{-4}$ sec^{-1}. The crystal was etched, pressurized at 0.35 GN m^{-2} re-etched, deformed and etched again.

To compare the dislocation substructures of deformed, but unpressurized and pressurized crystals, two nominally identical etched specimens were compressed. Only one had been pressurized at 0.35 GN m^{-2} and re-etched prior to testing. The stress-strain curves showed features already reported, in particular the unpressurized sample exhibited easy glide. Both compression tests were stopped at a strain of $\sim 0.6\%$ and the crystals were removed from the testing assembly and again etched.

The unpressurized crystal now exhibited a well developed glide band microstructure [10], whereas for the pressurized glide bands were absent (Fig. 8), except for the regions near the specimen compression faces. The dislocation density, however, had randomly but appreciably increased throughout the crystal, except in the immediate vicinities of the voids, where only a few new pits were observed. Examination of the crystal in transmitted polarized light indicated the general absence of extensive slip band structure, i.e. that the phenomenon was not confined to surface layers.

Detailed examination of Fig. 8 and other similar micrographs has failed to detect any movement of pressurization-induced dislocations during subsequent compression to stresses of the order of the yield stress of the material. In our LiF these dislocations were observed to have moved only when compressive strains of $\sim 6\%$ were applied when the shear stress reached ~ 10 MN m^{-2}, i.e. about five times the yield stress of unpressurized crystals. In a batch of (less pure) Harshaw LiF, however, numerous pressurization-induced dislocations were observed to have moved well below $\tau_y \sim 24$ MN m^{-2}, at stresses of ~ 12 MN m^{-2}.

The absence of slip band structure in compressed pressurized specimens was investigated further by detailed examination of the microstructure developed during compression. An as-annealed specimen was given a compressive strain of $\sim 0.1\%$ and lightly etched. Examination of {100} surfaces revealed the presence of fresh compression-induced dislocations, lying in the expected slip band configuration. The crystal was then pressurized at 0.75 GN m^{-2} and re-etched (Fig. 9a), followed by a further compressive strain of $\sim 0.3\%$ and another etch (Fig. 9b). It is seen that pressurization-induced dislocations, formed between the two compressions, had inhibited any further development of the glide bands produced by the initial 0.1% strain. Detailed examination of edge arrays after the pressurization and subsequent compression, e.g. Fig. 9b, failed to detect any dislocation movement from the glide bands, whereas many dislocations present in the original screw arrays (Fig. 9c) had moved. Again there was no evidence of any well defined arrays produced by dislocation movement during the 0.1 to 0.4% straining which followed the pressurization.

6. Discussion

It is through their effects on the plastic deformation that pressurization-induced dislocations

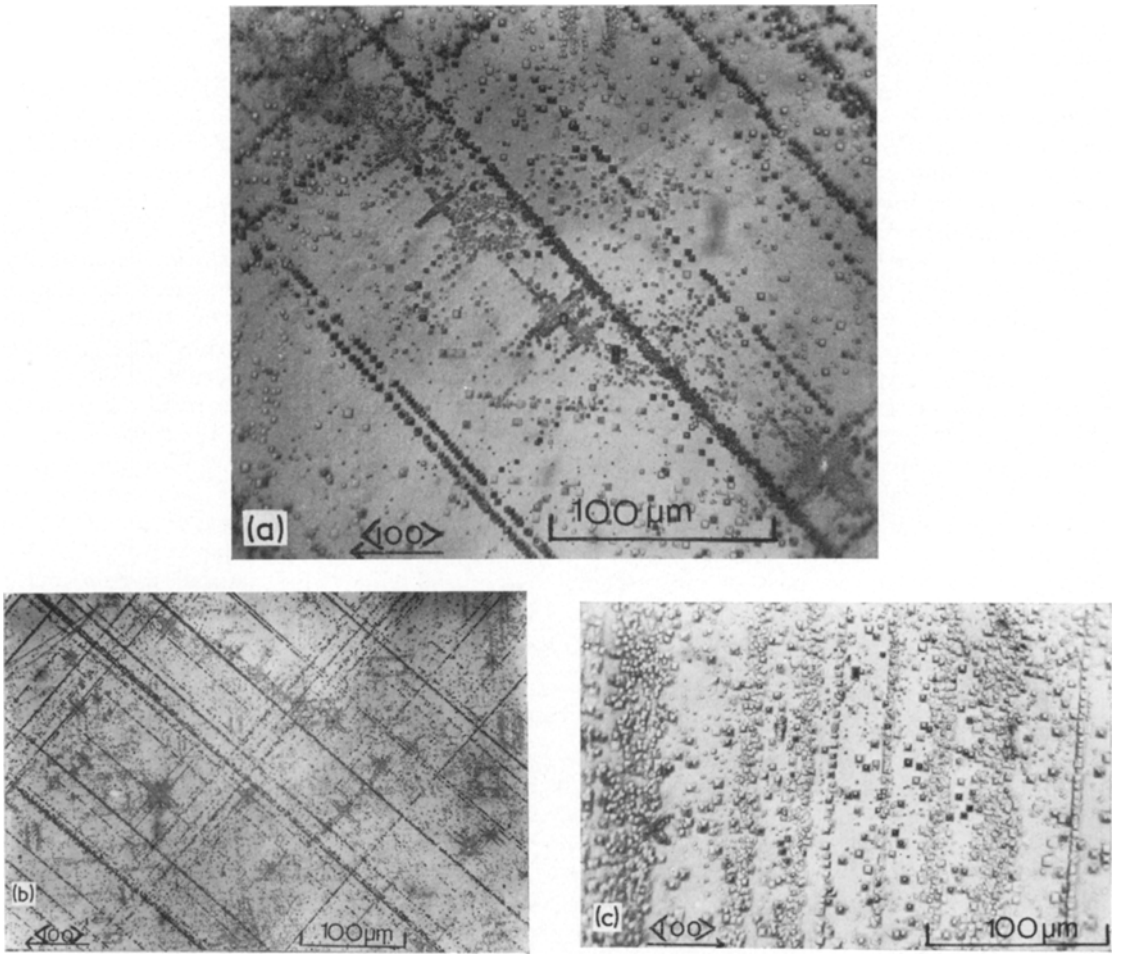

Figure 9 (a) Microstructure on a {100} face of a LiF single crystal which had been compressed ~ 0.1% at room temperature to initiate slip bands, pressurized at 0.75 GN m^{-2} and re-etched. (b) A micrograph of the same face following a further ~ 0.3% strain and etching. Note that glide band broadening had been prevented and there is no evidence of movement of pressurization-induced dislocations. (c) Microstructure of another {100} face, on which screw glide bands formed, after the same treatment as (b). Note that many dislocations produced by the first 0.1% compression had moved during restraining which followed the pressurization.

were first detected [13, 14, 16] in metals. The results presented in this communication indicate the general similarity of the effects in bcc metals and alkali halides. As the former possess five independent slip systems, prismatic punching [16] is favoured as the mechanism of dislocation nucleation; for NaCl, LiF and MgO [12], possessing only two independent slip systems, however, a simple slip process [11, 12] has been postulated.

In LiF the pressurization-induced dislocations, although on slip planes, formed relatively stable arrays and when treatment at higher pressures generated further slip, it was on other neighbouring planes. The microstructure present when pressurized crystals were compressed consisted of, effectively, deformed islands, schematically illustrated in Fig. 1b. When compression-induced flow started, slip bands were not able to form because the extent of obstacle-free slip plane available was restricted. With increasing pressurization treatment, for LiF, the volume of the available matrix decreased (Fig. 1b). It is worth noting at this point that as four slip systems appear to operate locally even at low strains, conjugate and oblique interactions become probable for the compression-induced dislocations, both with the pressurization-induced

arrays on all the six slip systems and with other compression-induced dislocations.

This situation thus resembles that of latent hardening in LiF and NaCl in that oblique interactions, jog formation [3] or dipoles [2] are thought to control the flow stress. In these experiments, however, it was found that the work hardening rate (in the hard direction) was substantially reduced, whereas, for LiF, pressurization increases it. To account for his observations Alden (for example) argued that only activation of orthogonal slip is necessary on two so far inactive systems on which it can then continue. This does not happen in our LiF crystals (Fig. 1) and, therefore, work hardening is expected to require further interactions and accordingly to increase, as observed (Fig. 6). The yield drop in LiF was suppressed by pressurization and, therefore [18], the mobile dislocation density at the commencement of macroscopic plastic flow in pressurized material is thought to have been increased from approximately 10^5 to $> 10^6$ cm^{-2} [19]. As a result of oblique interactions these dislocations may soon consist of many segments separated by jogs and sessile junctions. Therefore, although numerous, they would be unable to move far and contribute significantly to macroscopic flow in contrast to latent hardening. It is thus suggested that during the transition between the microstrain and the stage II regions of the stress-strain curves of pressurized crystals many intersections (both conjugate and oblique) are taking place. This transition for example, occurs in 0.4 and 0.7% plastic strain following pressurizations at 0.4 and 0.8 GN m^{-2} respectively. It is thought that the overall higher stress applied to the latter specimens is responsible for the increased extent of this region. As extensive movement and rapid multiplication of these fresh dislocations are inhibited, so is a yield point drop and easy glide. The increased stresses necessary to move jogged dislocations can give rise to the increase in the flow stress and to its dependence on the seasoning pressure. To summarize, glide bands cannot form in the pressurized LiF crystals and if introduced prior to the pressurization (Fig. 9) do not broaden during a subsequent compression. As a consequence, any further deformation, at an increased stress, must take place initially by the movement of the screw components of the glide loops. It is therefore suggested that in pressurized crystals dislocation behaviour in general, and interactions in particular, are of a different nature to those in stage I of unpressurized materials.

Gilman and Johnston [8] have shown that dislocation movement, at a given velocity, required a greater stress in a strained crystal than in an unstrained crystal. The extra stress required is approximately equal to the increase in flow stress of the hardened crystal. They further showed that dislocation density increased linearly with plastic strain and investigated the relationship between this stress increment and the dislocation density, $\Delta\tau/\rho$, using data from two different experiments. The calculation for the extra applied shear stress required to move screw dislocations at a given velocity in a strained crystal compared to that in an undeformed crystal yielded the value of $\sim$ 5 dyne per dislocation for $\Delta\tau/\rho$. Gilman and Johnston [8] also observed a linear relationship between the flow stress and glide band saturation density (for crystals of various hardnesses) which gave them a value of $\sim$ 3.7 dyne per dislocation. They concluded that specific dislocation reactions did not play an important role in strain hardening and suggested that defects, in the wakes of moving dislocations, interfere with subsequent dislocation glide on the same and neighbouring planes. This analysis is compatible with our results and the plot of τ_y versus pressurization-induced dislocation density (Fig. 5) gives a slope of 5 to 6 dyne per dislocation for τ/ρ, in fair agreement with Gilman and Johnston's values.

Acknowledgements

This work was supported by the Science Research Council and one of us (RAE) wishes also to acknowledge the award of a University of Bradford Studentship. We are grateful to Dr M. S. Stucke for stimulating discussions and to Professor D. Bijl for provision of laboratory facilities.

References

1. P. L. PRATT, *Acta Metallurgica* **1** (1953) 103.
2. R. W. DAVIDGE and P. L. PRATT, *Phys. Stat. Sol.* **6** (1964) 759.
3. T. H. ALDEN, *Trans. Met. Soc. AIME* **230** (1964) 649.
4. B. H. KEAR, C. E. SILVERSTONE and P. L. PRATT, *Proc. Brit. Ceram. Soc.* **6** (1966) 269.
5. R. W. DAVIDGE, *ibid* **6** (1966) 295.
6. J. C. M. LI, "Recrystallization, Grain Growth and Textures" (A.S.M., Metals Park, Ohio, 1966) p. 72.
7. Y. NAKADA and A. S. KEH, *Phys. Stat. Sol.* **32** (1969) 715.
8. J. J. GILMAN and W. G. JOHNSTON, *J. Appl. Phys.* **31** (1960) 687.

9. B. A. W. REDFERN, R. A. EVANS and A. S. WRONSKI, *J. Mater. Sci.* **5** (1970) 784.
10. R. A. EVANS, B. A. W. REDFERN and A. S. WRONSKI, *ibid* **7** (1972) 1216.
11. R. A. EVANS, A. S. WRONSKI and B. A. W. REDFERN, *Phil. Mag.* **29** (1974) 1381.
12. M. S. STUCKE and A. S. WRONSKI, *J. Mater. Sci.* **9** (1974) 911.
13. F. P. BULLEN, F. HENDERSON, M. M. HUTCHINSON and H. L. WAIN, *Phil. Mag.* **9** (1964) 285.
14. H. G. MELLOR and A. S. WRONSKI, *Acta Metallurgica* **19** (1970) 765.
15. A. S. WRONSKI, R. A. EVANS and B. A. W. REDFERN, in "Solids under Pressure", edited by H. Ll. Pugh (Inst. Mech. Eng., London, 1971) p. 94.
16. A. BALL and F. P. BULLEN, *Phil. Mag.* **22** (1970) 39.
17. H. BROOKS, "Metal Interfaces" (A.S.M., Metals Park, Ohio, 1962) p. 20.
18. J. J. GILMAN and W. G. JOHNSTON, *J. Appl. Phys.* **30** (1959) 129.
19. W. G. JOHNSTON, *J. Appl. Phys.* **33** (1962) 2716.

Received 29 August and accepted 9 September 1974.